Four Quadrant Torque Ripple Free Operation of BLDC Motor by Virtual Hall Signal Transitions at Phase Back EMF ZDPs

Umesh Kumar Soni, *Student Member IEEE*
Department of Electrical Engineering
Motilal Nehru National Institute of Technology
Allahabad, India
ree1456@mnnit.ac.in

Ramesh Kumar Tripathi, *Senior Member IEEE*
Department of Electrical Engineering
Motilal Nehru National Institute of Technology
Allahabad, India
rktripathi@mnnit.ac.in

***Abstract*— In the proposed work, the performance of complete control algorithm for the of Brushless DC motor has been evaluated using the virtual hall sensor transitions at the Zero Difference Points (ZDPs) of phase back EMFs, which are the zero crossing points of line to line back EMFs. The estimated line–to-line back EMF using Unknown Input Observer (UIO) has been directly converted to the hall signals which have transitions at ZDPs. The virtual hall sensor signals obtained from the proposed algorithm is similar to the actual hall signals but the proposed scheme is more sensitive during starting togetherwith speed and torque reversals during braking. Feed-forward torque and speed proportional control of phase currents have been implemented. The simulation study has been carried out for the validation. The proposed noise insensitive scheme provides excellent dynamic and steady state ripple free torque performance together with the zero speed starting capability.**

Index Terms-- Four Quadrant operation; BLDC motor; ZDP; Unknown Input Observer.

I. INTRODUCTION

Brushless DC motors are widely used in industries, aerospace, medical, electric vehicles and household purposes, due to its high efficiency and performance [1, 2]. The position information for the operation of the appropriate switches for optimal torque can be achieved either by shaft encoders or the hall sensors [3]. Recently, due to limitations of hall sensors and encoders, the sensorless techniques [4,5] such as diode freewheeling current detection [6-8], back EMF ZCP detection [9-20], third harmonic of back EMF detection [10, 20], back EMF integration till ZCP [20,21] were in use. Indirect method of back EMF detection by PWM needs neutral point. In improved direct back EMF detection, one side and two side chopping PWM strategies were also applied for the detection of back EMFs without neutral terminal [11]. Also in [12], two types of schemes are used, i.e. BEMF detection during PWM off time and BEMF detection during PWM on time. Introduction of PWM introduces large amount of noise in the sensed signal. Complementary PWM with the [17] helps in correction of offset voltage of back EMF signal due to diode voltage drop, but they can set up unwanted oscillations in torque and degrade the motor performance [11], [22]. The estimation based methods are preferred over detection based methods due to the delays and distortions involved in the detection based methods [18]. Reverse effect of detection circuit can propagate to on main circuit. Due to the programming possibility of the observer based complex control schemes through the high speed digital platforms like LABVIEW, DSP, FPGA etc., various observer based control techniques were introduced such as flux linkage estimation and variation, inductance variation, load observer, sliding mode observers, robust de-convolution filters, and robust stochastic observers have been implemented [23-31]. Various functions for the commutation of the switches were devised such as Speed Independent Position Function [34], Commutation Function [30], phase back EMF Zero crossing point (ZCP). Need of additional delay after ZCP has been overcome in the phase back EMF zero difference point (ZDP) detection based method introduced in [33]. The phase back EMF ZDP method has been implemented with estimated back EMF using unknown input observer in [34]. For applying these techniques for four quadrant operation of BLDC drive, virtual hall sensor transitions are needed, which can be generated from the observer based estimated line–to-line back EMFs. In the proposed work, the virtual hall signals transitions are generated at Zero Difference Point (ZDPs) of phase back EMFs. The ZDPs are situated at zero crossing point of line to line back EMF estimated from line voltages and currents using unknown input observer [29]. The method can control the BLDC drive in all four quadrant of operation.

II. MODELING OF BLDC MOTOR

A general schematic of VSI fed BLDC motor [33] is shown below in Figure 1. For validating the back EMF zero difference point detection method, we need to detect or

978-1-5386-1379-5/17/$31.00 ©2017 IEEE

estimate the back EMF first. The back EMF can be detected by unknown input observer [29]. The waveforms of hall sensor signals, back EMFs and phase currents [33] are shown in Figure 2.

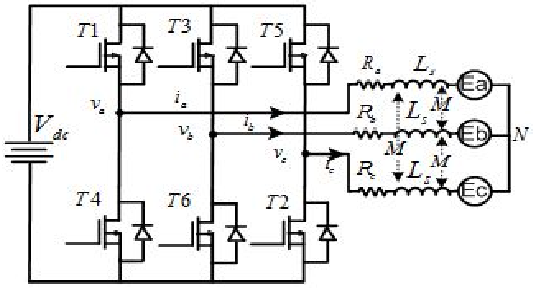

Figure 1 VSI fed BLDC motor.

The differential equation representation for all three phases of motor is given by,

$$v_a = R_a i_a + L_a \frac{di_a}{dt} + e_a + v_n \tag{1}$$

$$v_b = R_b i_b + L_b \frac{di_b}{dt} + e_b + v_n \tag{2}$$

$$v_c = R_c i_c + L_c \frac{di_c}{dt} + e_c + v_n \tag{3}$$

$$R = R_a = R_b = R_c, L = L_a = L_b = L_c = L_s - M \tag{4}$$

Effective torque as given by the equation below,

$$T_e = K_{T_1} Trapez(\theta_r + \frac{\pi}{2}) i_a(t) + K_{T_1} Trapez(\theta_r - \frac{2\pi}{3} + \frac{\pi}{2}) i_b(t) + K_{T_1} Trapez(\theta_r + \frac{2\pi}{3} + \frac{\pi}{2}) i_c(t) = T_a + T_b + T_c \tag{5}$$

The angular movement affects to changes the value of back EMFs as shown in eq(19-21),

$$e_a = K_{E_1} Trapez(\theta_r + \frac{\pi}{2}) \omega_r(t) \tag{6}$$

$$e_b = K_{E_1} Trapez(\theta_r - \frac{2\pi}{3} + \frac{\pi}{2}) \omega_r(t) \tag{7}$$

$$e_c = K_{E_1} Trapez(\theta_r + \frac{2\pi}{3} + \frac{\pi}{2}) \omega_r(t) \tag{8}$$

Trapez(.) = peicewise linear and periodic signal having trapezoidal shape with 2π angle rotor angle.

ω_r, θ_r = angular speed and position of the rotor.

$K_{E_1} = P\psi / 2$ = back EMF constant.

$K_{T_1} = P\psi / 2$ = Torque constant.

P = no. of poles.

ψ = magnitude of flux linkage of rotor magnet.

Speed achieved is given by,

$$T_e - T_L = J \frac{d\omega_r}{dt} + B\omega_r \tag{6}$$

The rotor angle can be calculated using

$$\theta_r = \int \hat{\omega}_r dt + \theta_0 \tag{7}$$

Where, θ_0 is initial angle of rotor with the phase-A axis and *Ke* is BEMF constant.

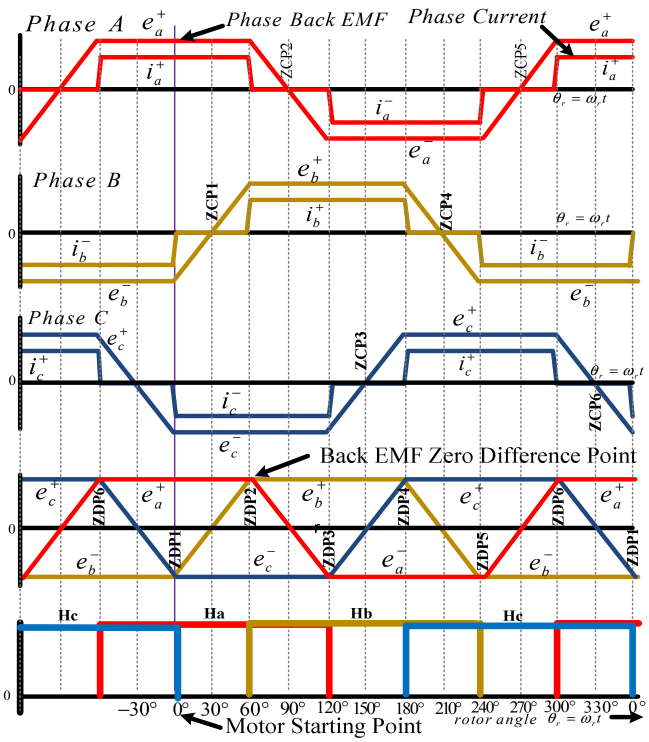

Figure 2 waveforms of phase currents and back EMF with hall signal transitions associated with ZDPs.

III. Back EMF Estimation for Getting ZDPs

Due to unavailability of the neutral point of motor, the phase back EMFs cannot be measured directly. So the phase to phase back EMF can be estimated from known phase currents and line voltages using the following equation,

$$\frac{d}{dt}(i_a - i_b) = -\frac{R}{L}(i_a - i_b) + \frac{1}{L}(v_a - v_b) - \frac{1}{L}(e_a - e_b) \tag{9}$$

Similarly for other phase groups also, the equations can be written. The quantities $v_a - v_b$, i_a, i_b in Eq.(3) are known state variables as they can be measured. The phase to phase back EMF $e_a - e_b$ is unknown disturbance quantity. The above equation can be written in state space matrix form as,

$$\dot{x} = Ax + Bu + Fw \tag{10}$$

Where $A = \left[-\frac{R}{L}\right], B = \left[\frac{1}{L}\right], F = \left[-\frac{1}{L}\right]$

$$x=[i_a-i_b],\ u=\left[v_a-v_b\right],\ w=[e_a-e_b],$$
$$y=[i_a-i_b], C=[1]$$

The unknown disturbance in phase to phase back EMF can be determined by the augmented state space matrix representation as below:

$$\dot{x}_a = A_a x_a + B_a u \tag{11}$$

$$y = C_a x_a \tag{12}$$

Where, $x_a = \begin{bmatrix} i_a - i_b \\ e_a - e_b \end{bmatrix}, u=[v_a - v_b], y=[i_a - i_b]$ and

$$A_a = \begin{bmatrix} -\frac{R}{L} & -\frac{1}{L} \\ 0 & 0 \end{bmatrix}, B_a = \begin{bmatrix} \frac{1}{L} \\ 0 \end{bmatrix}, C_a = [1\ \ 0]$$

System in Eq. (11) and Eq. (12) being the observable system, it is possible to compose the complete state space given by Eq.(14) in the form of the following observer,

$$\dot{\hat{x}}_a = A_a \hat{x}_a + B_a u + K(y-\hat{y}) \tag{13}$$

$$\frac{d}{dt}\begin{bmatrix} \hat{i}_a-\hat{i}_b \\ \hat{e}_a-\hat{e}_b \\ \hat{i}_b-\hat{i}_{cn} \\ \hat{e}_b-\hat{e}_c \\ \hat{i}_c-\hat{i}_a \\ \hat{e}_c-\hat{e}_a \end{bmatrix} = \begin{bmatrix} -\frac{R}{L} & -\frac{1}{L} & 0 & 0 & 0 & 0 \\ 0 & 0 & 0 & 0 & 0 & 0 \\ 0 & 0 & -\frac{R}{L} & -\frac{1}{L} & 0 & 0 \\ 0 & 0 & 0 & 0 & 0 & 0 \\ 0 & 0 & 0 & 0 & -\frac{R}{L} & -\frac{1}{L} \\ 0 & 0 & 0 & 0 & 0 & 0 \end{bmatrix} \begin{bmatrix} \hat{i}_a-\hat{i}_b \\ \hat{e}_a-\hat{e}_b \\ \hat{i}_b-\hat{i}_c \\ \hat{e}_b-\hat{e}_c \\ \hat{i}_c-\hat{i}_a \\ \hat{e}_c-\hat{e}_a \end{bmatrix} + \begin{bmatrix} \frac{1}{L} & 0 & 0 \\ 0 & 0 & 0 \\ 0 & \frac{1}{L} & 0 \\ 0 & 0 & 0 \\ 0 & 0 & \frac{1}{L} \\ 0 & 0 & 0 \end{bmatrix} \begin{bmatrix} v_a-v_b \\ v_b-v_c \\ v_c-v_c \end{bmatrix} + \begin{bmatrix} K_1 & 0 & 0 \\ K_2 & 0 & 0 \\ 0 & K_3 & 0 \\ 0 & K_4 & 0 \\ 0 & 0 & K_5 \\ 0 & 0 & K_6 \end{bmatrix} \begin{bmatrix} \varepsilon_{iab} \\ \varepsilon_{ibc} \\ \varepsilon_{ica} \end{bmatrix} \tag{14}$$

Where, $\varepsilon_{iab} = (i_a - i_b) - (\hat{i}_a - \hat{i}_b)$ is the estimation error in line current obtained from phase currents in phase-A and phase-B. Similarly other estimation errors can also be defined. Block diagram of the proposed scheme with observer has been shown in Figure 3.

IV. VIRTUAL HALL SIGNAL LOGIC

For four quadrant application, virtual hall sensor signal generation has been in practice. Depending on the value of the estimated line to line back EMF the virtual hall signal transitions are obtained at the corresponding phase back EMF Zero Difference Points (ZDPs). The virtual Hall Signal value and the ZDPs relative to the line-to-line back EMFs are explained in the Figure 4. The logic of virtual hall sensor signal generation has been given in Table.1.

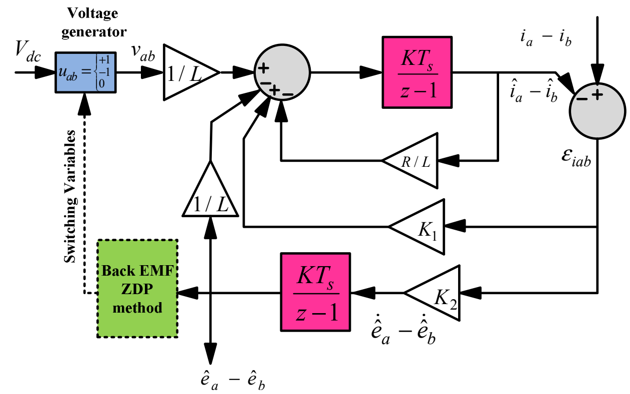

Figure 3 proposed Sensorless Control.

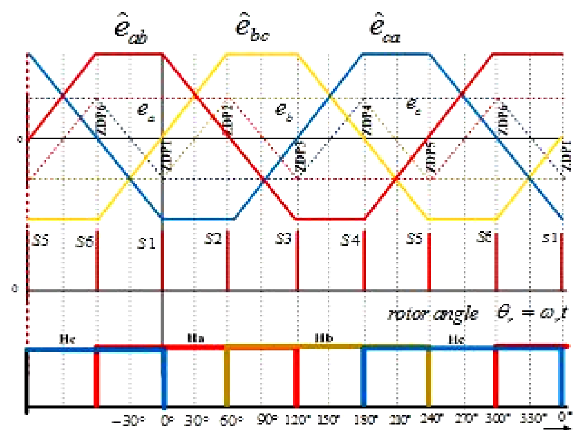

Figure 4 Virtual Hall Sensor signals at phase back EMF ZDPs.

TABLE.1 VIRTUAL HALL SIGNALS RELATIVE TO PHASE BACK EMF ZDPS AND LINE-TO-LINE BEMF

Phase BEMF ZDPs	Line-to-Line Back EMF	Value of Line-to -Line BEMF	Virtual Hall Signal
ZDP1-ZDP4	Ebc	Positive	Hc=0
ZDP2-ZDP5	Eab	Negative	Hb=1
ZDP3-ZDP6	Eca	Positive	Ha=0
ZDP4-ZDP1	Ebc	Negative	Hc=1
ZDP5-ZDP2	Eab	Positive	Hb=0
ZDP6-ZDP3	Eca	Negative	Ha=1

V. PROPOSED SENSORLESS FOUR-QUADRANT SYSTEM.

In the proposed four quadrant control, the magnitude of current proportional to reference speed is controlled by current controller comprised of PI and hysteresis controllers. During the reversal of rotation, the back EMFs vary in opposite sequence. So if the direction of reference speed is greater and actual speed is less than zero (or vice-versa) then the current reference is negative. When the motor starts to run in the required direction after crossing zero speed, current reference again becomes positive, while the hall sequence is in opposite direction due to reversed BEMF sequence. The virtual hall signals at Zero difference points (ZDPs) of phase back EMFs are fed to switches. A torque proportional feed forward controller improves the dynamic performance. Current limiter provides the facility of limiting the starting torque within permissible limit. The six signals for switches are fed to the rectangular current generator and the PWM is generated for each switch from a PI and hysteresis controller. Complete controller structure has been shown in Figure 5(a) and 5(b). The logic for the virtual hall signals and current references for various modes have been shown in Table 2 and Table 3.

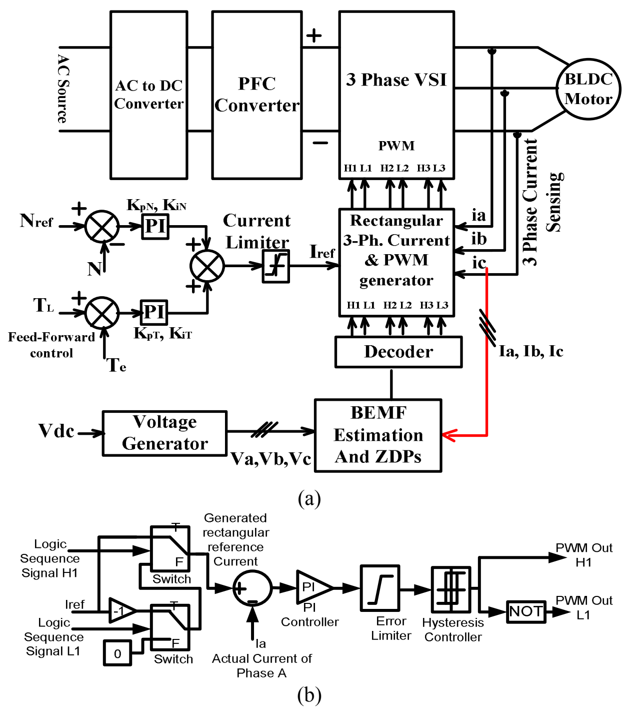

Figure 5 (a) proposed sensorless four quadrant control system (b) PWM generated by comparing the generated rectangular reference current to the actual current of phase A.

TABLE.2 REFERENCE CURRENT, REFERENCE SPEED AND ACTUAL SPEED FOR DIFFERENT MODES OF FOUR QUADRANT OPERATION

Mode of Operation	Reference Speed	Actual Speed	Current Reference	Sequence of Hall Signals
Forward Motoring	Positive	Positive	Positive	Positive
Forward Breaking	Negative	Positive	Negative	Positive
Reverse Motoring	Negative	Negative	Positive	Negative
Reverse Braking	Positive	Negative	Negative	Negative

TABLE.3 SEQUENCE OF LINE-TO-LINE BEMF AND VIRTUAL HALL SIGNALS DURING REVERSE AND FORWARD MOTORING

Sequences	Reverse Motoring	Forward Motoring
Line-to-Line Back EMF	*Eab – Eca –Ebc - Eab*	*Eab – Ebc – Eca - Eab*
Corresponding Hall Signals	*Hb – Ha – Hc - Ha*	*Hb – Hc – Ha - Hb*

VI. PERFORMANCE EVALUATION

The performance of the proposed four quadrant brushless DC motor using the virtual hall sensor signal transitions generated at the zero difference points of phase back EMF is evaluated using the MATLAB/Simulink. The simulation parameters of motor and controller for simulation are shown in Table.4.

TABLE.4 MOTOR AND CONTROLLER PARAMETERS

Motor Parameter	Value
Per Phase Inductance	8.5mH
Per phase Resistance	2.875 ohm
Voltage Constant	49 VpeakL_L / Krpm
Torque Constant	0.46792 Nm/A-peak
Flux linkage by rotor magnets	0.23396 V.sec
Rotor Inertia	0.0008 kg.m^2
Viscous damping	0.001 N.m.sec
Pole Pairs	1
Nominal DC link voltage Vdc	300 Volt DC
Kalman gain K1	3500
Kalman Gain K2	-100000
Forward Gain K	1
Threshold for phase back EMF ZDP	$V_{dc}/1500$
Hysteresis band	0.000005
PWM generator Kp, Ki	0.00005, 0.00000005
Torque proportional control KpT , KiT	1.075, 0.000005
Speed Proportional Control KpN,KiN	0.006, 0.000006
Saturation	0.000006
Current limiter	20,-20

In first case the reference (or load) torque is 5 Nm and reference speed is 1000 rpm from 0-0.15 s. The reference load becomes zero with reference speed of -2000 rpm at 0.15 s. After 0.25 s the reference (or load) torque is still zero with reference speed of 500 rpm. The performance is shown in Figure 6. Corresponding speed and torque trajectory (i.e. magnitude vs. rotor angle polar plot) has been shown in Figure 7 (a) and Figure 7 (b). The line-to-line BEMF with the corresponding hall signals during four quadrant operation has been shown in Figure 8.

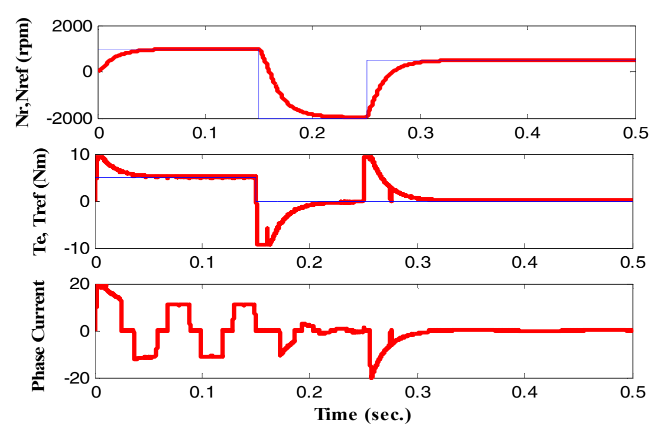

Figure 6 Speed reference versus achieved speed, reference load torque versus developed electromagnetic torque and the phase current.

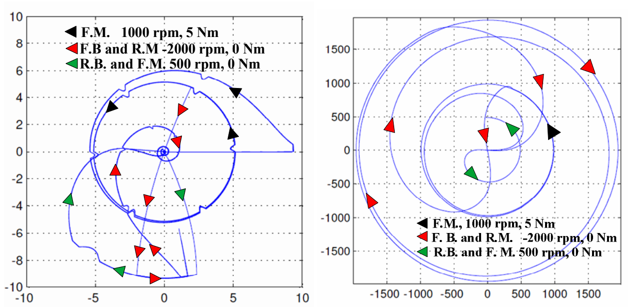

Figure 7 (a) Torque trajectory (polar plot of magnitude vs rotor angle) represents the reversal during forward braking and reverse braking (axes in Nm). (b) Speed trajectory representing the reversal during forward braking and reverse braking (axes in RPM).

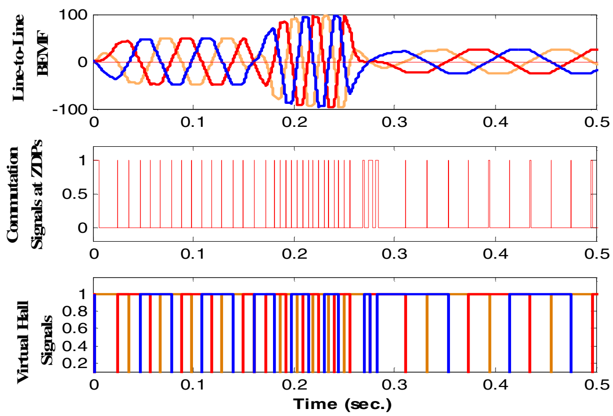

Figure 8 estimated line to line back EMF, commutation signals at ZDPs and virtual hall signals generated. (red-Eab, Hb; yellow–Ebc, Hc; blue-Eca, Ha).

In the next case as shown in Fig. 9, the performance has been evaluated while the initial reference speed is -1000 and reference torque is -2 Nm (reverse motoring) at starting. Again, speed reference changes to 2000 rpm with reference torque of 5Nm at 0.3 s. At the instant 0.5 s, speed reference changes to 500 rpm with 5 Nm reference torque. The torque and speed trajectory is shown in Figure 10(a) and Figure 10(b). The line-to-line BEMF with the corresponding hall signals during four quadrant operation for the second case has been shown in Figure 11.

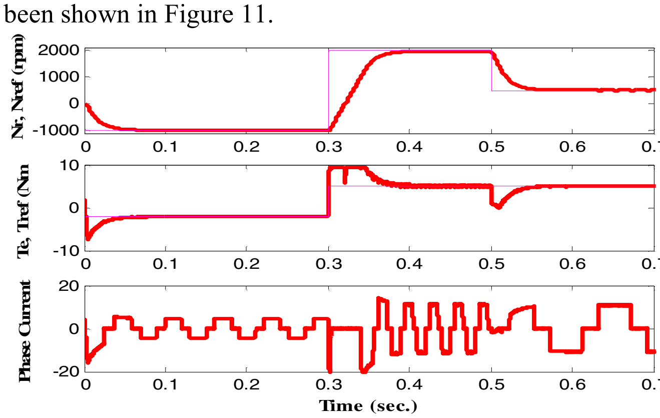

Figure 9 Speed reference versus achieved speed, reference load torque versus developed electromagnetic torque, and the phase current.

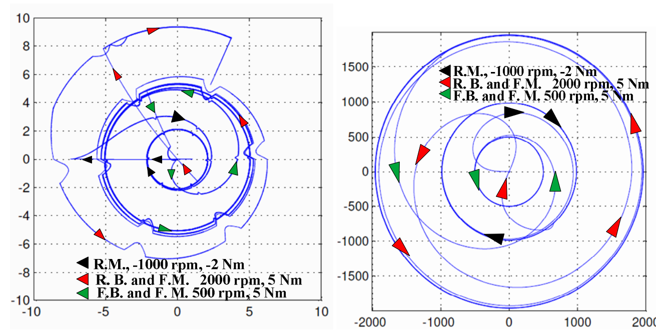

Figure 10 (a) Torque trajectory (polar plot) representing the reversal during forward braking and reverse braking (axes in Nm). (b) Speed trajectory (polar plot) representing the reversal during forward braking and reverse braking (axes in RPM).

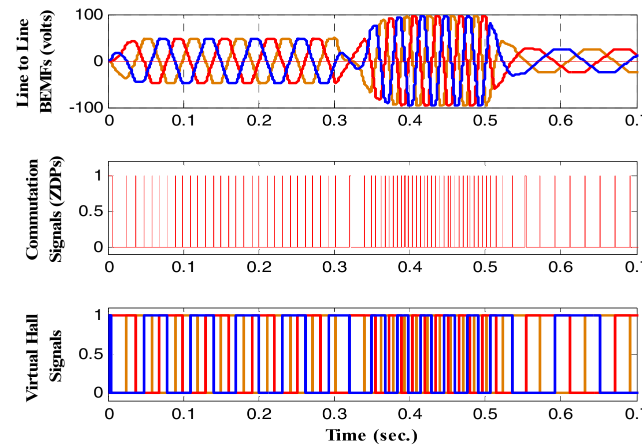

Figure 11 estimated line to line back EMF, commutation signals at ZDPs and virtual hall signals generated. (red-Eab, Hb; yellow–Ebc, Hc; blue-Eca, Ha).

VII. Conclusion

The performance of the proposed four-quadrant sensorless position control of brushless DC motor based on the estimated line to line back EMF using Unknown input observer has been investigated. The virtual hall sensor signal transitions were obtained at the zero difference points (ZDPs) of the phase back EMFs. The proposed scheme has excellent performance at various load and torque references. The method is self starting due to the reason that it provides the switching pulses based on the noise comparison of back EMFs during standstill and starts the initial movement. The current limiter, current controller and feed forward torque proportional current controller has enhanced the performance in terms of fast response and reduced torque ripple and excellent reference tracking. So the proposed sensorless four quadrant scheme proves to be a best alternative to the real hall sensor and encoder based control.

Acknowledgement

The whole research work is being encouraged by Motilal Nehru National Institute of Technology Allahabad, UP, India and is supported by Vishveshwaraiya PhD scheme under the ESDM sector of Department of Electronics and Information Technology, Ministry of Electronics and Information Technology, Govt. of India as an initiative of Digital India.

REFERENCES

[1] M.V.Kesava Rao, Department of Electrical technology, IISc Bangalore, "*Brush Contact Drops in DC machines",* Accepted 25-6-1934, Bangalore Press.

[2] Y.S. Jeon, H.S. Mok, G.H. Choe, D.K. Kim, J.S. Ryu, "A New Simulation Model of BLDC Motor with Real Back EMF waveform", *Proc. 7 th workshop on Computers in power Electronics* (COMPEL 2000), page 217-220.

[3] Padmaja yedmale, "Brushless DC (BLDC) Motor Fundamentals", AN885, 2003 Microchip Technology.

[4] J. R. Frus and B. C. Kuo, "Closed-loop control of step motors using waveform detection," in Proc. Int. Conf. Stepping Motors and Systems, Leeds, U.K., 1976, pp. 77–84.

[5] S. Tara , Syfullah Khan Md "Simulation of sensorless operation of BLDC motor based on the zero cross detection from the line voltage" International Journal of Advanced Research in Electrical Electronics and Instrumentation Engineering, vol 2, issue 12 , December 2013, ISSN 2320-3765.

[6] R. L. Lin, M. T. Hu, S. C. Chen and C. Y. Lee, "Using phase-current sensing circuit as the position sensor for brushless DC motors without shaft position sensor," *15th Annual Conference of IEEE Industrial Electronics Society*, Philadelphia, PA, 1989, pp. 215-218 vol.1.

[7] S. Ogasawara and H. Akagi, "An approach to position sensorless drives for brushless DC motors", *IEEE Trans. On Industry Applications* vol.27, no.5 pp.928-933, 1991.

[8] Ching-Guo Chen, Tian-Hua Liu, Ming-Tsan Lin and Chih-An Tai, "Position control of a sensorless synchronous reluctance motor," *in IEEE Transactions on Industrial Electronics, vol. 51, no. 1, pp. 15-25, Feb. 2004.*

[9] K. Iizuka, H. Uzuhashi, and M. Kano, "Microcomputer control for sensorless brushless motor," IEEE Trans. on Industry Applications, vol. 27, pp. 595-601, 1985.

[10] J.C. Moreira, "Indirect sensing for rotor flux position of permanent magnet AC motors operating over the wide speed range", *IEEE trans. on Industry Applications*, vol. 32, no. 6, pp. 1394-1401, 1996.

[11] J. Shao, D. Nolan, and T. Hopkins, "A novel direct back EMF detection for sensorless brushless DC(BLDC) motor drives," *17th Annual IEEE Applied Power Electronics Conference and Exposition,* Vol. 1, pp. 33-37, Mar. 2002.

[12] Application note "back emf detection during PWM on time by T7MC" AN2030, STM Electronics.

[13] Q. Jiang, C. Bi, and R. Huang, "A new phase delay- free method to detect back EMF zero crossing points for sensorless control of spindle motors," IEEE Trans. Magn., vol. 41, no. 7, pp.2287-2294, 2005.

[14] Y. Kang, S. B. Lee, and J. Yoo, "A microcontroller embedded AD converter based low coast sensorless technique for brushless dc motor drives," *IEEE Conf. Industry Applications*, Vol. 3, pp. 2176-2181, Oct. 2005.

[15] C. G. Kim, J. H. Lee, H. W. Kim, and M. J. Youn, "Study on maximum torque generation for sensorless controlled brushless dc motor with trapezoidal back EMF," *IEE Proceedings of Electric Power Applications,* Vol.152, Issue 2, pp. 277-291, Mar. 2005.

[16] Lei Zhang, Wei Xiao and Wenlong Qu, "Sensorless Control of BLDC Motors Using an Improved Low-cost Back EMF Detection Method", *37th IEEE Power Electronics Specialists conference PECS*, 2006.

[17] Yushui, Yugang Xin, Weicheng Zhang, "An improved BEMF Detection Method for sensorless BLDC motor" *IEEE international conference in Industrial technology*, ICIT 2008.

[18] P. Damodharan and Krishna Vasudevan, "Sensorless Brushless DC Motor Drive Based on the Zero-Crossing Detection of Back Electromotive Force (EMF) from the Line Voltage Difference", *IEEE Trans on energy conversion*, vol. 25, no. 3, September 2010.

[19] Lai Y.-S. Lin Y.-K., "A unified approach to zero crossing point detection of back EMF for Brushless DC motor drives without current and hall sensors". *IEEE Trans. Power Electron.* 26(6), 2011).

[20] T.M. Jahns, R.C. Becerra, and M. Ehsani, "Integrated current regulation for a brushless ECM drive", *IEEE trans. on power Electronics*, Vol No. 6, No.1, pp 118-126, 1991.

[21] H.R Anderson and J.K. Pedersen, "Sensorless ELBERFELD control of brushless DC motors for energy optimized variable speed household refrigerators," *Proc. 7th European conference on Power electronics and applications*, vol.1, pp. 314-318, 1997.

[22] J. X. Shen, K. J. Tseng, "Analyses and Compensation of Rotor Position Detection Error in Sensorless PM Brushless DC Motor Drives," *IEEE Trans. Energy Conversion,* vol. 18, no. 1, pp. 87-93,March 2003.

[23] Fakham H, Djemai M, Busawon K. "Design and practical implementation of a back-EMF sliding-mode observer for a brushless DC motor", *IET Electr. Power Appl.* 2008;2(6):353–61.

[24] R. Wu and G. R. Slemon, "A permanent magnet motor drive without a shaft sensor," *IEEE Transactions on Industry Application*, vol. 27, pp. 1005–1011, Sept. /Oct. 1991.

[25] N. Ertugrul and P. Acarnley, "A new algorithm for sensorless operation of permanent magnet motors," *IEEE Trans. Ind. Applicat.*, vol. 30, pp. 126–133, Jan./Feb. 1994.

[26] J. S. Kim, and S. K. Sul, "New approach for high-performance PMSM drives without rotational position sensors," *IEEE Trans. Power Electronics*, Vol. 12, pp. 904-911, Sep. 1997.

[27] Jium –Ming Lin , Ming –Chang Lin, Hsin –Ping Wang, "LEQG/LTR controller design with extended kalman filter for sensorless brushless DC driver.", *Computer. Methods Applied Mechanical Engineering* 190(2001) pp.5481-5494, Elsevier.

[28] Ki- hong Park, tae-Sung Kim, Sung-Chan Ahn, Dong-Seok Hyun, "Speed Control of High Performance Brushless DC Motor drives by load Torque Estimation", *34th IEEE Power Electronics Specialist Conference,* 2003 PECS 03, pp. 1677-1681.

[29] Tae-Sung Kim,Byong –Gun Park, Dong-Myung Lee, Ji-su Ryu and Dong –Seok Hyun, "A new Approach to sensorless control method for brushless DC Motors", *International Journal of Control Automation and Systems,* vol. 6 No.4 PP 477-487, August 2008.

[30] S.A.KH. Mozaffari Niapour, M. Tabarraie , M.R. Feyzi, "Design and analysis of speed-sensorless robust stochastic L_∞ -induced observer for high-performance brushless DC motor drives with diminished torque ripple" *Energy Conversion and Management,* 64 (2012) 482–498.

[31] S.A.KH. Mozaffari Niapour, M. Tabarraie , M.R. Feyzi, "A new robust speed sensorless control strategy for high performance brushless DC motor drives with reduced torque ripple", *Control Engineering Practice(Elsevier),* 24(2014), 42-54.

[32] Tae-Hyung Kim ,M. Ehsani, "Sensorless control of BLDC motors from near zero to high speeds", IEEE Transactions on Power Electonics , ISSN 0885-8993,vol 19, No. 6, p.1635-1645, Nov 2004.

[33] U mesh Kumar Soni and Ramesh Kumar Tripathi, "Novel Back EMF Zero Difference Point Detection Based Sensorless Technique for BLDC Motor", *Proceedings of IEEE 18th Annual International Conference on Industrial Technology,* ICIT 2017, 22-25 March 2017, Toronto, Canada, pp.330-335.

[34] Umesh Kumar Soni and Ramesh Kumar Tripathi, "Novel estimated Back EMF ZDP based Sensorless Controlled BLDCM using Unknown Input Observer", unpublished, *Proc. IEEE International Seminar on Intelligent Technologies and Its Application, Surabaya, Indonesia*, pp.121-126.